



Observations of $B_s^0 \rightarrow \psi(2S)\eta$ and $B_{(s)}^0 \rightarrow \psi(2S)\pi^+\pi^-$ decays [☆]

LHCb Collaboration

Received 27 February 2013; accepted 8 March 2013

Available online 13 March 2013

Abstract

First observations of the $B_s^0 \rightarrow \psi(2S)\eta$, $B^0 \rightarrow \psi(2S)\pi^+\pi^-$ and $B_s^0 \rightarrow \psi(2S)\pi^+\pi^-$ decays are made using a dataset corresponding to an integrated luminosity of 1.0 fb^{-1} collected by the LHCb experiment in proton–proton collisions at a centre-of-mass energy of $\sqrt{s} = 7 \text{ TeV}$. The ratios of the branching fractions of each of the $\psi(2S)$ modes with respect to the corresponding J/ψ decays are

$$\frac{\mathcal{B}(B_s^0 \rightarrow \psi(2S)\eta)}{\mathcal{B}(B_s^0 \rightarrow J/\psi\eta)} = 0.83 \pm 0.14 \text{ (stat)} \pm 0.12 \text{ (syst)} \pm 0.02 \text{ (}\mathcal{B}\text{)},$$

$$\frac{\mathcal{B}(B^0 \rightarrow \psi(2S)\pi^+\pi^-)}{\mathcal{B}(B^0 \rightarrow J/\psi\pi^+\pi^-)} = 0.56 \pm 0.07 \text{ (stat)} \pm 0.05 \text{ (syst)} \pm 0.01 \text{ (}\mathcal{B}\text{)},$$

$$\frac{\mathcal{B}(B_s^0 \rightarrow \psi(2S)\pi^+\pi^-)}{\mathcal{B}(B_s^0 \rightarrow J/\psi\pi^+\pi^-)} = 0.34 \pm 0.04 \text{ (stat)} \pm 0.03 \text{ (syst)} \pm 0.01 \text{ (}\mathcal{B}\text{)},$$

where the third uncertainty corresponds to the uncertainties of the dilepton branching fractions of the J/ψ and $\psi(2S)$ meson decays.

© 2013 CERN. Published by Elsevier B.V. All rights reserved.

1. Introduction

Decays of B mesons containing a charmonium resonance, J/ψ or $\psi(2S)$, in the final state play a crucial role in the study of CP violation and in the precise measurement of neutral B meson mixing parameters.

[☆] © CERN for the benefit of the LHCb Collaboration.

The $B_s^0 \rightarrow J/\psi \eta$ decay was observed by the Belle Collaboration and the branching fraction was measured to be $\mathcal{B}(B_s^0 \rightarrow J/\psi \eta) = (5.10 \pm 0.50 \pm 0.25^{+1.14}_{-0.79}) \times 10^{-4}$ [1], where the first uncertainty is statistical, the second systematic and the third due to the uncertainty in the number of produced $B_s^0 \bar{B}_s^0$ pairs. This decay has also recently been reported by LHCb, including the decay $B_s^0 \rightarrow J/\psi \eta'$ [2].

The $B_{(s)}^0 \rightarrow J/\psi \pi^+ \pi^-$ decays, where $B_{(s)}^0$ denotes a B^0 or B_s^0 meson, have been studied previously and the $\pi^+ \pi^-$ final states are found to comprise the decay products of the $\rho^0(770)$ and $f_2(1270)$ mesons in case of B^0 decays and of $f_0(980)$ and $f_0(1370)$ mesons in case of B_s^0 decays [3–5]. The B_s^0 modes have been used to measure mixing-induced CP violation [6,7]. The decays $B_s^0 \rightarrow \psi(2S)\eta$ and $B_{(s)}^0 \rightarrow \psi(2S)\pi^+ \pi^-$ have not previously been studied.

The relative branching fractions of B^0 and B_s^0 mesons into final states containing J/ψ and $\psi(2S)$ mesons have been studied by several experiments (CDF [8,9], D0 [10] and LHCb [11]). In this paper, measurements of the branching fraction ratios of $B_{(s)}^0$ mesons decaying to $\psi(2S)X^0$ and $J/\psi X^0$ are reported, where X^0 denotes either an η meson or a $\pi^+ \pi^-$ system. Charge conjugate decays are implicitly included. The analysis presented here is based on a data sample corresponding to an integrated luminosity of 1.0 fb^{-1} collected with the LHCb detector during 2011 in pp collisions at a centre-of-mass energy of $\sqrt{s} = 7 \text{ TeV}$.

2. LHCb detector

The LHCb detector [12] is a single-arm forward spectrometer covering the pseudorapidity range $2 < \eta < 5$, designed for the study of particles containing b or c quarks. The detector includes a high precision tracking system consisting of a silicon-strip vertex detector surrounding the pp interaction region, a large-area silicon-strip detector located upstream of a dipole magnet with a bending power of about 4 Tm, and three stations of silicon-strip detectors and straw drift tubes placed downstream. The combined tracking system has momentum resolution $\Delta p/p$ that varies from 0.4% at 5 GeV/c to 0.6% at 100 GeV/c, and impact parameter resolution of 20 μm for tracks with high transverse momentum (p_T). Charged hadrons are identified using two ring-imaging Cherenkov detectors. Photon, electron and hadron candidates are identified by a calorimeter system consisting of scintillating-pad and preshower detectors, an electromagnetic calorimeter and a hadronic calorimeter. Muons are identified by a system composed of alternating layers of iron and multiwire proportional chambers.

The trigger [13] consists of a hardware stage, based on information from the calorimeter and muon systems, followed by a software stage where a full event reconstruction is applied. Candidate events are first required to pass a hardware trigger which selects muons with a transverse momentum, $p_T > 1.48 \text{ GeV}/c$. In the subsequent software trigger, at least one of the final state particles is required to have both $p_T > 0.8 \text{ GeV}/c$ and impact parameter $> 100 \mu\text{m}$ with respect to all of the primary pp interaction vertices (PVs) in the event. Finally, two or more of the final state particles are required to form a vertex which is significantly displaced from the PVs.

For the simulation, pp collisions are generated using PYTHIA 6.4 [14] with a specific LHCb configuration [15]. Decays of hadronic particles are described by EVTGEN [16] in which final state radiation is generated using PHOTOS [17]. The interaction of the generated particles with the detector and its response are implemented using the GEANT4 toolkit [18,19] as described in Ref. [20].

3. Event selection

The decays $B_{(s)}^0 \rightarrow \psi\eta$ and $B_{(s)}^0 \rightarrow \psi\pi^+\pi^-$, where ψ denotes J/ψ or $\psi(2S)$, are reconstructed using $\psi \rightarrow \mu^+\mu^-$ and $\eta \rightarrow \gamma\gamma$ decay modes. Pairs of oppositely-charged tracks identified as muons, each having $p_T > 0.55$ GeV/ c and originating from a common vertex, are combined to form $\psi \rightarrow \mu^+\mu^-$ candidates. Track quality is ensured by requiring the χ^2 per number of degrees of freedom (χ^2/ndf) provided by the track fit to be less than 5. Well identified muons are selected by requiring that the difference in logarithms of the global likelihood of the muon hypothesis, $\Delta \log \mathcal{L}_{\mu h}$ [21], provided by the particle identification detectors, with respect to the hadron hypothesis is larger than zero. The fit of the common two-prong vertex is required to satisfy $\chi^2/\text{ndf} < 20$. The vertex is deemed to be well separated from the reconstructed primary vertex of the proton–proton interaction by requiring the decay length significance to be larger than three. Finally, the invariant mass of the dimuon combination is required to be between 3.020 and 3.135 GeV/ c^2 for J/ψ candidates and between 3.597 and 3.730 GeV/ c^2 for $\psi(2S)$ candidates. These correspond to $[-5\sigma; 3\sigma]$ intervals around the nominal masses to accommodate QED radiation.

The pions are required to have $p_T > 0.25$ GeV/ c and an impact parameter χ^2 , defined as the difference between the χ^2 of the PV formed with and without the considered track, larger than 9. When more than one PV is reconstructed, the smallest value of impact parameter χ^2 is chosen. In addition, to suppress contamination from kaons, the difference between the logarithms of likelihoods of the pion and kaon hypotheses, $\Delta \log \mathcal{L}_{\pi K}$ [22], provided by the RICH detectors, has to be larger than zero.

Photons are selected from neutral clusters in the electromagnetic calorimeter with transverse energy in excess of 0.4 GeV. The $\eta \rightarrow \gamma\gamma$ candidates are reconstructed as diphoton combinations with an invariant mass within ± 70 MeV/ c^2 of the η mass [23]. To suppress the large combinatorial background from the decays of neutral pions, photons that form a $\pi^0 \rightarrow \gamma\gamma$ candidate with invariant mass within ± 25 MeV/ c^2 of the π^0 mass are not used to reconstruct $\eta \rightarrow \gamma\gamma$ candidates.

The $B_{(s)}^0$ candidates are formed from ψX^0 combinations. In the $\psi\eta$ case an additional requirement $p_T(\eta) > 2.5$ GeV/ c is applied to reduce combinatorial background. To improve the invariant mass resolution a kinematic fit [24] is performed. In this fit, constraints are applied on the known masses [23] of intermediate resonances, and it is also required that the candidate's momentum vector points to the associated primary vertex. The χ^2/ndf for this fit is required to be less than 5. Finally, the decay time, ct , of the $B_{(s)}^0$ candidate, calculated with respect to the primary vertex, is required to be in excess of 150 μm .

4. Observation of the $B_s^0 \rightarrow \psi(2S)\eta$ decay

The invariant mass distributions of the selected $\psi\eta$ candidates are shown in Fig. 1. The $B_s^0 \rightarrow \psi\eta$ signal yields are estimated by performing unbinned extended maximum likelihood fits. The B_s^0 signal is modelled by a Gaussian distribution and the background by an exponential function. In the $J/\psi\eta$ case a possible contribution from the corresponding B^0 decays is included in the fit model as an additional Gaussian component. The resolutions of the two Gaussian functions are set to be the same and the difference of their central values is fixed to the known difference between the B_s^0 and the B^0 masses [23]. The contribution from the decay $B^0 \rightarrow \psi(2S)\eta$ is not considered in the baseline fit model. The mass resolution of the

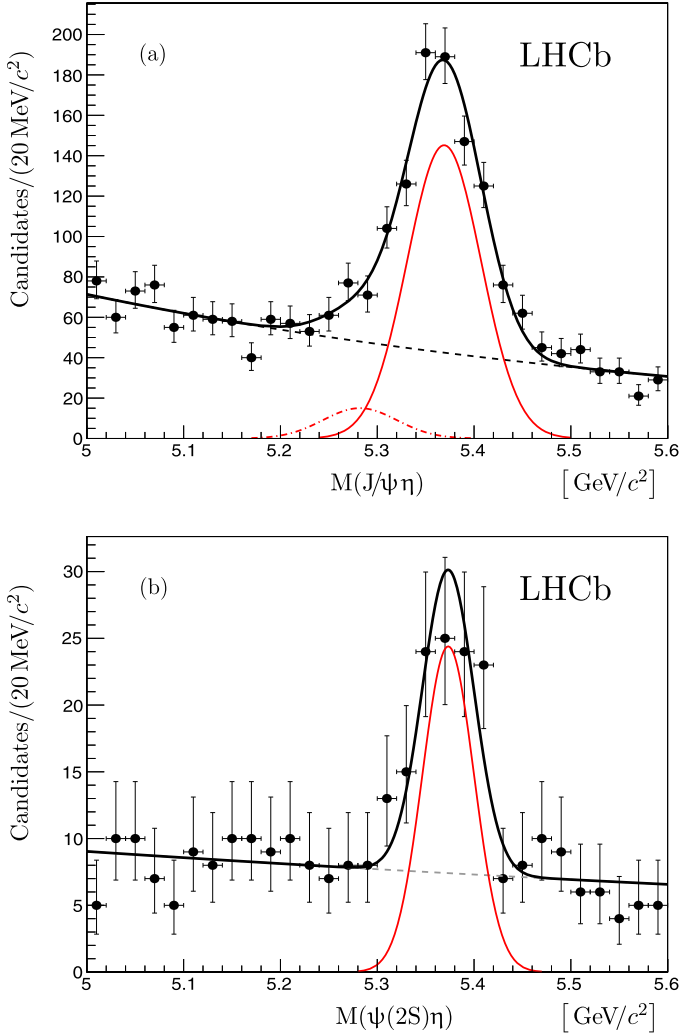


Fig. 1. Mass distributions of (a) $B_s^0 \rightarrow J/\psi \eta$ and (b) $B_s^0 \rightarrow \psi(2S) \eta$ candidates. The total fit function (solid black) and the combinatorial background (dashed) are shown. The solid red lines show the signal B_s^0 contribution and the red dot dashed line corresponds to the B^0 contribution. (For interpretation of the references to colour in this figure legend, the reader is referred to the web version of this article.)

$B_s^0 \rightarrow \psi(2S) \eta$ decay mode is fixed to the value $\sigma_{\text{DATA}}^{\psi(2S)\eta} = \sigma_{\text{DATA}}^{J/\psi\eta} \times \sigma_{\text{MC}}^{\psi(2S)\eta} / \sigma_{\text{MC}}^{J/\psi\eta}$, where σ_{DATA} and σ_{MC} are the widths of the corresponding channel in data and simulation, respectively.

The fit results are summarised in Table 1. In all cases the positions of the signal peaks are consistent with the nominal B_s^0 mass [23] and the resolutions are in agreement with the expectations from simulation. The measured yield of $B^0 \rightarrow J/\psi \eta$ is 144 ± 41 events (uncertainty is statistical only), which is consistent with the expected value based on the measured branching fraction of this decay [25]. The statistical significance in each fit is determined as $S = \sqrt{-2 \ln \frac{\mathcal{L}_B}{\mathcal{L}_{S+B}}}$, where \mathcal{L}_{S+B} and \mathcal{L}_B denote the likelihood of the signal plus background hypothesis and the

Table 1

Fitted values of signal events (N_B), signal peak position (M_B) and resolution (σ_B). The quoted uncertainties are statistical only.

Mode	N_B	M_B [MeV/ c^2]	σ_B [MeV/ c^2]
$B_s^0 \rightarrow J/\psi \eta$	863 ± 52	5370.9 ± 2.3	33.7 ± 2.3
$B_s^0 \rightarrow \psi(2S) \eta$	76 ± 12	5373.4 ± 5.0	26.6 fixed

Table 2

Fitted values of signal events (N_B), signal peak position (M_B) and resolution (σ_B). The quoted uncertainties are statistical only.

Mode	N_B	M_B [MeV/ c^2]	σ_B [MeV/ c^2]
$B^0 \rightarrow J/\psi \pi^+ \pi^-$	2801 ± 85	5281.1 ± 0.3	8.2 ± 0.3
$B_s^0 \rightarrow J/\psi \pi^+ \pi^-$	4096 ± 86	5368.4 ± 0.2	8.7 ± 0.2
$B^0 \rightarrow \psi(2S) \pi^+ \pi^-$	202 ± 23	5280.3 ± 1.0	8.4 ± 1.1
$B_s^0 \rightarrow \psi(2S) \pi^+ \pi^-$	178 ± 22	5366.3 ± 1.2	9.1 ± 1.4

background only hypothesis, respectively. Taking into account the systematic uncertainty related to the fit function, which is discussed in detail in Section 6, the significance of the $B_s^0 \rightarrow \psi(2S) \eta$ signal is 6.2σ .

To demonstrate that the signal originates from $B_s^0 \rightarrow \psi(2S) \eta$ decays the *sPlot* technique [26] has been used to separate the signal and the background. Using the $\mu^+ \mu^- \gamma \gamma$ invariant mass distribution as the discriminating variable, the distributions for the invariant masses of the intermediate resonances $\eta \rightarrow \gamma \gamma$ and $\psi(2S) \rightarrow \mu^+ \mu^-$ have been obtained. In this procedure, the invariant mass window for each corresponding resonance is released and the mass constraint is removed. The resulting invariant mass distributions for $\gamma \gamma$ and $\mu^+ \mu^-$ from $B_s^0 \rightarrow \psi(2S) \eta$ candidates are shown in Fig. 2. Clear signals are seen in both $\eta \rightarrow \gamma \gamma$ and $\psi(2S) \rightarrow \mu^+ \mu^-$ decays. The distributions are described by the sum of a Gaussian function and a constant. The fit shows that the constant is consistent with zero, as expected.

5. Observation of the $B_{(s)}^0 \rightarrow \psi(2S) \pi^+ \pi^-$ decays

The invariant mass distributions for the $B_{(s)}^0 \rightarrow \psi \pi^+ \pi^-$ candidates are shown in Fig. 3. The narrow signals correspond to the $B^0 \rightarrow \psi \pi^+ \pi^-$ and $B_s^0 \rightarrow \psi \pi^+ \pi^-$ decays. The peak at lower mass corresponds to a reflection from $B^0 \rightarrow \psi K^{*0} (\rightarrow K^+ \pi^-)$ decays where the kaon is misidentified as a pion. The contribution from $B_s^0 \rightarrow \psi K^{*0}$ decays [27] is negligible.

The invariant mass distributions are fitted with two Gaussian functions to describe the two signals, an asymmetric Gaussian function with different width for the two sides to represent the reflection from $B^0 \rightarrow \psi K^{*0}$ decays and an exponential function for the background. The fit results are summarised in Table 2. The statistical significances of the signals are found to be larger than 9 standard deviations.

For the $B_{(s)}^0 \rightarrow J/\psi \pi^+ \pi^-$ decays, the $\pi^+ \pi^-$ mass shapes have been studied in detail using a partial wave analysis in Refs. [4,5]. The main contributions are $B^0 \rightarrow J/\psi \rho^0(770)$ and $B_s^0 \rightarrow J/\psi f_0(980)$. However, due to the limited number of signal events, the same method cannot be used for the $B_{(s)}^0 \rightarrow \psi(2S) \pi^+ \pi^-$ decays. The *sPlot* technique is used in order to study the dipion

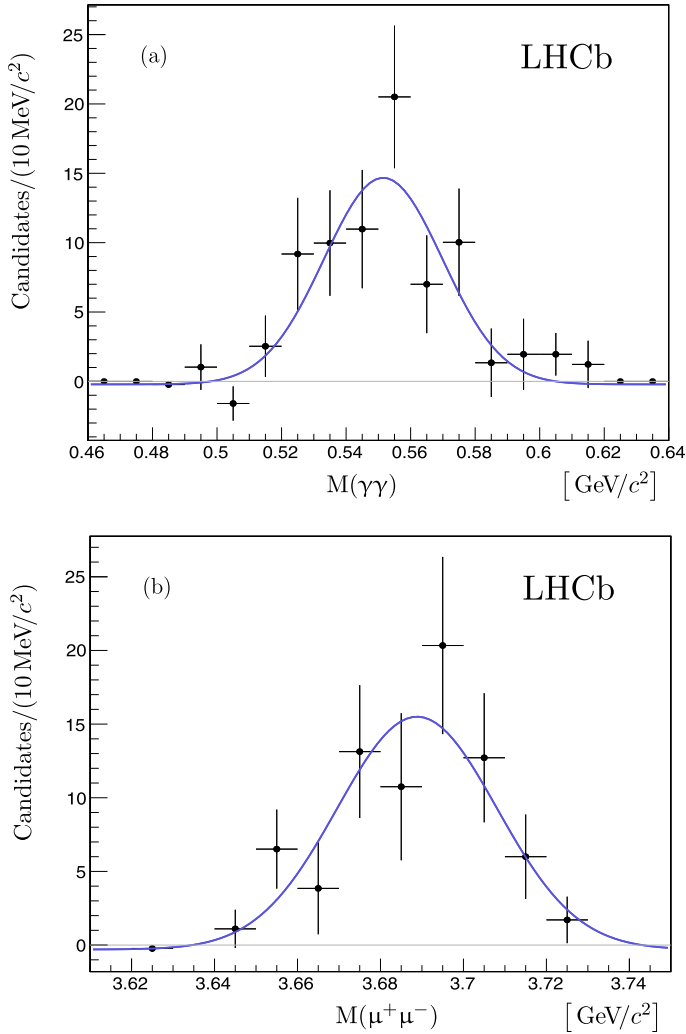


Fig. 2. Background subtracted (a) $\gamma\gamma$ and (b) $\mu^+\mu^-$ mass distributions in $B_s^0 \rightarrow \psi(2S)\eta$ decays. In both cases the blue line is the result of the fit described in the text. (For interpretation of the references to colour in this figure legend, the reader is referred to the web version of this article.)

mass distribution in those decays. With the $\psi(2S)\pi^+\pi^-$ invariant mass as the discriminating variable, the $\pi^+\pi^-$ invariant mass spectra from $B_{(s)}^0 \rightarrow \psi(2S)\pi^+\pi^-$ decays are obtained (see Fig. 4).

To check that the background subtracted $\pi^+\pi^-$ distributions have similar shapes in both channels, the distribution obtained from the $\psi(2S)\pi^+\pi^-$ decay is fitted with the distribution obtained from the $J/\psi\pi^+\pi^-$ channel, corrected by the ratio of phase-space factors and by the ratio of the efficiencies which depends on the dipion invariant mass. The p-value for the χ^2 fit is 30% for $B^0 \rightarrow \psi\pi^+\pi^-$ and 7% for $B_s^0 \rightarrow \psi\pi^+\pi^-$, respectively. As seen in Fig. 4, $B^0 \rightarrow \psi(2S)\rho^0(770)$ and $B_s^0 \rightarrow \psi(2S)f_0(980)$ decays are the main contributions to $B_{(s)}^0 \rightarrow \psi(2S)\pi^+\pi^-$ decays. Detailed amplitude analyses of the resonance structures in $B_{(s)}^0 \rightarrow \psi(2S)\pi^+\pi^-$ decays, similar to

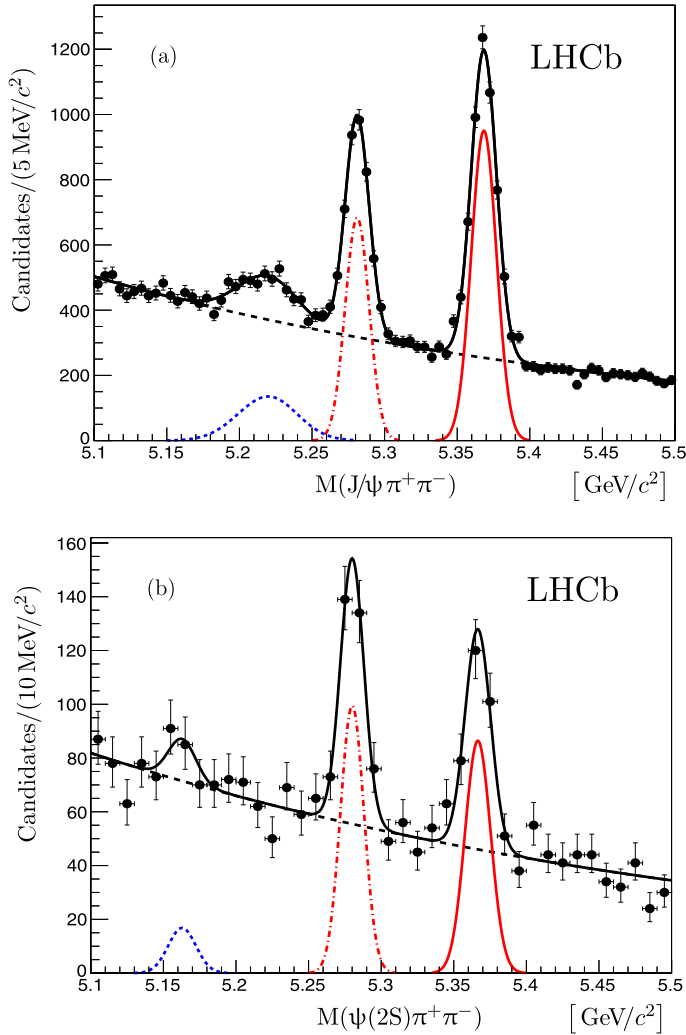


Fig. 3. Mass distributions of (a) $B_{(s)}^0 \rightarrow J/\psi \pi^+ \pi^-$ and (b) $B_{(s)}^0 \rightarrow \psi(2S) \pi^+ \pi^-$ candidates. The total fit function (solid black) and the combinatorial background (dashed) are shown. The solid red lines show the signal $B_{(s)}^0$ contribution and the red dot dashed lines correspond to the B^0 contributions. The reflections from misidentified $B^0 \rightarrow \psi K^{*0}$, $K^{*0} \rightarrow K^+ \pi^-$ decays are shown with dotted blue lines. (For interpretation of the references to colour in this figure legend, the reader is referred to the web version of this article.)

Refs. [4,5], will be possible with a larger dataset. This will allow the possible excess of events in the region $M(\pi^+ \pi^-) > 1.4 \text{ GeV}/c^2$ to be investigated.

The narrow peak around $0.5 \text{ GeV}/c^2$ in Fig. 4(a) is dominated by $K_S^0 \rightarrow \pi^+ \pi^-$ from $B^0 \rightarrow J/\psi K_S^0$ decays. The contributions from K_S^0 decays are taken into account by the fit function described in Ref. [2]. The resulting yields are 129 ± 26 in the J/ψ channel and 11 ± 6 in the $\psi(2S)$ channel. In the calculation of the final ratio of branching fractions, the number of K_S^0 events is subtracted from the corresponding $B^0 \rightarrow \psi \pi^+ \pi^-$ yields. The yield from $B_s^0 \rightarrow \psi K_S^0$ decays is negligible [28].

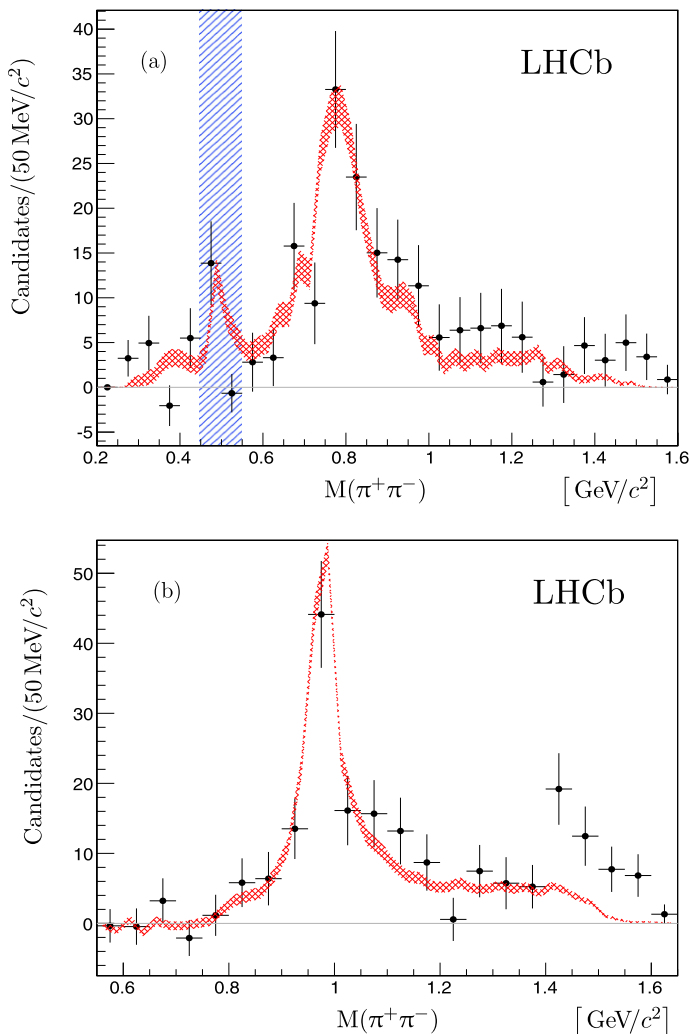


Fig. 4. Background subtracted $\pi^+\pi^-$ mass distribution in (a) $B^0 \rightarrow \psi(2S)\pi^+\pi^-$ and (b) $B_s^0 \rightarrow \psi(2S)\pi^+\pi^-$ (black points). The red filled area shows the expected signal spectrum for the $\psi(2S)$ channel derived from the measured spectrum of the J/ψ channel (the fit has one parameter—the normalisation). The width of the band corresponds to the uncertainties of the distribution from the J/ψ channel. In case of $B^0 \rightarrow \psi(2S)\pi^+\pi^-$, the blue vertical filled area shows the K_S^0 region that is excluded from the fit. (For interpretation of the references to colour in this figure legend, the reader is referred to the web version of this article.)

6. Efficiencies and systematic uncertainties

The ratios of branching fractions are calculated using the formula

$$\frac{\mathcal{B}(B \rightarrow \psi(2S)X^0)}{\mathcal{B}(B \rightarrow J/\psi X^0)} = \frac{N_{\psi(2S)X^0}}{N_{J/\psi X^0}} \times \frac{\epsilon_{J/\psi X^0}}{\epsilon_{\psi(2S)X^0}} \times \frac{\mathcal{B}(J/\psi \rightarrow \mu^+\mu^-)}{\mathcal{B}(\psi(2S) \rightarrow \mu^+\mu^-)}, \quad (1)$$

where N is the number of signal events, and ϵ is the product of the geometrical acceptance, the detection, reconstruction, selection and trigger efficiencies. The efficiency ratios are estimated using simulation for all six decay modes.

The efficiency ratios are 1.22 ± 0.01 , 1.03 ± 0.01 and 1.02 ± 0.01 for the $B_s^0 \rightarrow \psi\eta$, $B^0 \rightarrow \psi\pi^+\pi^-$ and $B_s^0 \rightarrow \psi\pi^+\pi^-$ channels, respectively (uncertainties are statistical only). Since the selection criteria for the decays with J/ψ and $\psi(2S)$ are identical, the ratio of efficiencies is expected to be close to unity. The deviation of the overall efficiency ratio from unity in case of $B_s^0 \rightarrow \psi\eta$ is due to the difference between the p_T spectra of the selected J/ψ and $\psi(2S)$ mesons, when the $p_T(\eta) > 2.5$ GeV/ c requirement is applied. For the $B_{(s)}^0 \rightarrow \psi\pi^+\pi^-$ channels this effect is small since no explicit p_T requirement is applied on the dipion system.

Most systematic uncertainties cancel in the ratio of branching fractions, in particular, those related to the muon and ψ reconstruction and identification. Systematic uncertainties related to the fit model are estimated using a number of alternative models for the description of the invariant mass distributions. For the $B_s^0 \rightarrow \psi\eta$ decays the tested alternatives are a fit model including a B^0 signal component (with the ratio $N(B^0 \rightarrow \psi\eta)/N(B_s^0 \rightarrow \psi\eta)$ fixed from the J/ψ channel), a fit model with a linear function for the background description, fits with signal widths fixed or not fixed to those obtained in simulation, a fit with the difference between the fitted B^0 and B_s^0 masses allowed to vary within a $\pm 1\sigma$ interval around the nominal value [23], and a fit model with Student's t -distributions for the signals. For each alternative fit model the ratio of event yields is calculated and the systematic uncertainty is then determined as the maximum deviation of this ratio from the ratio obtained with the baseline model. For $B_{(s)}^0 \rightarrow \psi\pi^+\pi^-$ decays the tested alternatives include a fit with a first or second order polynomial for the background description, a model with a symmetric Gaussian distribution for the reflection and a model with the difference of the mean values of the two Gaussian functions fixed to the known mass difference between the B_s^0 and the B^0 mesons [23]. The maximum deviation observed in the ratio of yields in the $\psi(2S)$ and J/ψ modes is taken as the systematic uncertainty. The obtained uncertainties are 8.0% for the $B_s^0 \rightarrow \psi\eta$ channel, 1.0% for the $B^0 \rightarrow \psi\pi^+\pi^-$ channel and 1.6% for the $B_s^0 \rightarrow \psi\pi^+\pi^-$ channel.

The selection efficiency for the dipion system has a dependence on the dipion invariant mass. The ratios of efficiencies vary over the entire $\pi^+\pi^-$ mass range by approximately 40% and 24% for $B^0 \rightarrow \psi\pi^+\pi^-$ and $B_s^0 \rightarrow \psi\pi^+\pi^-$ channels, respectively. The systematic uncertainties related to the different dependence of the efficiency as a function of the dipion invariant mass for J/ψ and $\psi(2S)$ channels are evaluated using the decay models from Ref. [5] for B_s^0 and Refs. [2,4] for B^0 decays. The systematic uncertainties on the branching fraction ratios are 2% for both channels.

The most important source of uncertainty arises from potential disagreement between data and simulation in the estimation of efficiencies. This source of uncertainty is studied by varying the selection criteria in ranges corresponding to approximately 15% change in the signal yields. The agreement is estimated by comparing the efficiency corrected ratio of yields with these variations. The resulting uncertainties are found to be 11.5% in the $B_s^0 \rightarrow \psi\eta$ channel and 8% in the $B_{(s)}^0 \rightarrow \psi\pi^+\pi^-$ channel.

The geometrical acceptance is calculated separately for different magnet polarities. The observed difference in the efficiency ratios is taken as an estimate of the systematic uncertainty and is 1.1% for the $B^0 \rightarrow \psi\pi^+\pi^-$ channel and negligible for the other channels.

The trigger is highly efficient in selecting B meson decays with two muons in the final state. For this analysis the dimuon pair is required to trigger the event. Differences in the trigger efficiency between data and simulation are studied in the data using events that were triggered independently of the dimuon pair [11]. Based on these studies, an uncertainty of 1.1% is assigned. A summary of all systematic uncertainties is presented in Table 3.

Table 3

Relative systematic uncertainties (in %) of the relative branching fractions.

Source	$B_s^0 \rightarrow \psi \eta$	$B^0 \rightarrow \psi \pi^+ \pi^-$	$B_s^0 \rightarrow \psi \pi^+ \pi^-$
Fit model	8.0	1.0	1.6
Mass dependence of efficiencies	–	2.0	2.0
Efficiencies from simulation	11.5	8.0	8.0
Acceptance	< 0.5	1.1	< 0.5
Trigger	1.1	1.1	1.1
Sum in quadrature	14.1	8.5	8.5

7. Results

With data corresponding to an integrated luminosity of 1.0 fb^{-1} , collected in 2011 with the LHCb detector, the first observations of the $B_s^0 \rightarrow \psi(2S)\eta$ and $B_{(s)}^0 \rightarrow \psi(2S)\pi^+\pi^-$ decays have been made. The relative rates of $B_{(s)}^0$ meson decays into final states containing J/ψ and $\psi(2S)$ mesons are measured for those decay modes. Since the dielectron branching fractions of ψ mesons are measured more precisely than those of the dimuon decay modes, invoking lepton universality, the ratio $\frac{\mathcal{B}(J/\psi \rightarrow \mu^+\mu^-)}{\mathcal{B}(\psi(2S) \rightarrow \mu^+\mu^-)} = \frac{\mathcal{B}(J/\psi \rightarrow e^+e^-)}{\mathcal{B}(\psi(2S) \rightarrow e^+e^-)} = 7.69 \pm 0.19$ [23] is used. The results are combined using Eq. (1), to give

$$\begin{aligned} \frac{\mathcal{B}(B_s^0 \rightarrow \psi(2S)\eta)}{\mathcal{B}(B_s^0 \rightarrow J/\psi \eta)} &= 0.83 \pm 0.14 \text{ (stat)} \pm 0.12 \text{ (syst)} \pm 0.02 \text{ (}\mathcal{B}\text{)}, \\ \frac{\mathcal{B}(B^0 \rightarrow \psi(2S)\pi^+\pi^-)}{\mathcal{B}(B^0 \rightarrow J/\psi \pi^+\pi^-)} &= 0.56 \pm 0.07 \text{ (stat)} \pm 0.05 \text{ (syst)} \pm 0.01 \text{ (}\mathcal{B}\text{)}, \\ \frac{\mathcal{B}(B_s^0 \rightarrow \psi(2S)\pi^+\pi^-)}{\mathcal{B}(B_s^0 \rightarrow J/\psi \pi^+\pi^-)} &= 0.34 \pm 0.04 \text{ (stat)} \pm 0.03 \text{ (syst)} \pm 0.01 \text{ (}\mathcal{B}\text{)}, \end{aligned}$$

where the first uncertainty is statistical, the second systematic and the third from the world average ratio [23] of the J/ψ and $\psi(2S)$ branching fractions to dileptonic final states. The branching fraction ratios measured here correspond to the time integrated quantities. For the $B^0 \rightarrow J/\psi(\psi(2S))\pi^+\pi^-$ channel the measured ratio excludes the $K_S^0 \rightarrow \pi^+\pi^-$ contribution. The dominant contributions to the $B_{(s)}^0 \rightarrow \psi(2S)\pi^+\pi^-$ decays are found to be from $B^0 \rightarrow \psi(2S)\rho^0(770)$ and $B_s^0 \rightarrow \psi(2S)f_0(980)$ decays.

These results are compatible with the measured range of relative branching fractions of B decays to $\psi(2S)$ and J/ψ mesons. The $B_s^0 \rightarrow \psi(2S)\eta$ and $B_s^0 \rightarrow \psi(2S)\pi^+\pi^-$ decays are particularly interesting since, with more data becoming available, they can be used to measure CP violation in B_s^0 mixing.

Acknowledgements

We express our gratitude to our colleagues in the CERN accelerator departments for the excellent performance of the LHC. We thank the technical and administrative staff at the LHCb institutes. We acknowledge support from CERN and from the national agencies: CAPES, CNPq, FAPERJ and FINEP (Brazil); NSFC (China); CNRS/IN2P3 and Region Auvergne (France); BMBF, DFG, HGF and MPG (Germany); SFI (Ireland); INFN (Italy); FOM and NWO (The Netherlands); SCSR (Poland); ANCS/IFA (Romania); MinES, Rosatom, RFBR and

NRC “Kurchatov Institute” (Russia); MinECo, XuntaGal and GENCAT (Spain); SNSF and SER (Switzerland); NAS Ukraine (Ukraine); STFC (United Kingdom); NSF (USA). We also acknowledge the support received from the ERC under FP7. The Tier1 computing centers are supported by IN2P3 (France), KIT and BMBF (Germany), INFN (Italy), NWO and SURF (The Netherlands), PIC (Spain), GridPP (United Kingdom). We are thankful for the computing resources put at our disposal by Yandex LLC (Russia), as well as to the communities behind the multiple open source software packages that we depend on.

Open access

This article is published Open Access at sciencedirect.com. It is distributed under the terms of the Creative Commons Attribution License 3.0, which permits unrestricted use, distribution, and reproduction in any medium, provided the original authors and source are credited.

References

- [1] Belle Collaboration, J. Li, et al., First observation of $B_s^0 \rightarrow J/\psi \eta$ and $B_s^0 \rightarrow J/\psi \eta'$, Phys. Rev. Lett. 108 (2012) 181808, arXiv:1202.0103.
- [2] LHCb Collaboration, R. Aaij, et al., Evidence for the decay $B^0 \rightarrow J/\psi \omega$ and measurement of the relative branching fractions of B_s^0 meson decays to $J/\psi \eta$ and $J/\psi \eta'$, Nucl. Phys. B 867 (2013) 547, arXiv:1210.2631.
- [3] LHCb Collaboration, R. Aaij, et al., First observation of $B_s^0 \rightarrow J/\psi f_0(980)$ decays, Phys. Lett. B 698 (2011) 115, arXiv:1102.0206.
- [4] LHCb Collaboration, R. Aaij, et al., Analysis of the resonant components in $B^0 \rightarrow J/\psi \pi^+ \pi^-$, Phys. Rev. D 87 (2013) 052001, <http://dx.doi.org/10.1103/PhysRevD.87.052001>, arXiv:1301.5347.
- [5] LHCb Collaboration, R. Aaij, et al., Analysis of the resonant components in $B_s^0 \rightarrow J/\psi \pi^+ \pi^-$, Phys. Rev. D 86 (2012) 052006, arXiv:1204.5643.
- [6] LHCb Collaboration, R. Aaij, et al., Measurement of the CP violating phase ϕ_s in $B_s^0 \rightarrow J/\psi f_0(980)$, Phys. Lett. B 707 (2012) 497, arXiv:1112.3056.
- [7] LHCb Collaboration, R. Aaij, et al., Measurement of the CP -violating phase ϕ_s in $B_s^0 \rightarrow J/\psi \pi^+ \pi^-$ decays, Phys. Lett. B 713 (2012) 378, arXiv:1204.5675.
- [8] CDF Collaboration, F. Abe, et al., Observation of $B^+ \rightarrow \psi(2S)K^+$ and $B^0 \rightarrow \psi(2S)K^{*0}(892)$ decays and measurements of B meson branching fractions into J/ψ and $\psi(2S)$ final states, Phys. Rev. D 58 (1998) 072001, arXiv:hep-ex/9803013.
- [9] CDF Collaboration, A. Abulencia, et al., Observation of $B_s^0 \rightarrow \psi(2S)\phi$ and measurement of ratio of branching fractions $\mathcal{B}(B_s^0 \rightarrow \psi(2S)\phi)/\mathcal{B}(B_s^0 \rightarrow J/\psi\phi)$, Phys. Rev. Lett. 96 (2006) 231801, arXiv:hep-ex/0602005.
- [10] D0 Collaboration, V. Abazov, et al., Relative rates of B meson decays into $\psi(2S)$ and J/ψ mesons, Phys. Rev. D 79 (2009) 111102, arXiv:0805.2576.
- [11] LHCb Collaboration, R. Aaij, et al., Measurement of relative branching fractions of B decays to $\psi(2S)$ and J/ψ mesons, Eur. Phys. J. C 72 (2012) 2118, arXiv:1205.0918.
- [12] LHCb Collaboration, A.A. Alves Jr., et al., The LHCb detector at the LHC, JINST 3 (2008) S08005.
- [13] R. Aaij, et al., The LHCb trigger and its performance, JINST, submitted for publication, arXiv:1211.3055.
- [14] T. Sjöstrand, S. Mrenna, P. Skands, PYTHIA 6.4 physics and manual, JHEP 0605 (2006) 026, arXiv:hep-ph/0603175.
- [15] I. Belyaev, et al., Handling of the generation of primary events in GAUSS, the LHCb simulation framework, Nucl. Sci. Symp. Conf. Rec. (NSS/MIC) IEEE (2010) 1155.
- [16] D.J. Lange, The EvtGen particle decay simulation package, Nucl. Instrum. Meth. A 462 (2001) 152.
- [17] P. Golonka, Z. Was, PHOTOS Monte Carlo: a precision tool for QED corrections in Z and W decays, Eur. Phys. J. C 45 (2006) 97, arXiv:hep-ph/0506026.
- [18] GEANT4 Collaboration, S. Agostinelli, et al., GEANT4: A simulation toolkit, Nucl. Instrum. Meth. A 506 (2003) 250.
- [19] GEANT4 Collaboration, J. Allison, et al., GEANT4 developments and applications, IEEE Trans. Nucl. Sci. 53 (2006) 270.
- [20] M. Clemencic, et al., The LHCb simulation application, GAUSS: design, evolution and experience, J. of Phys. Conf. Ser. 331 (2011) 032023.

- [21] A.A. Alves, et al., Performance of the LHCb muon system, JINST 8 (2013) P02002, <http://dx.doi.org/10.1088/1748-0221/8/02/P02002>, arXiv:1211.1346.
- [22] M. Adinolfi, et al., Performance of the LHCb RICH detector at the LHC, Eur. Phys. J., submitted for publication, arXiv:1211.6759.
- [23] Particle Data Group, J. Beringer, et al., Review of particle physics, Phys. Rev. D 86 (2012) 010001.
- [24] W.D. Hulsbergen, Decay chain fitting with a Kalman filter, Nucl. Instrum. Meth. A 552 (2005) 566, arXiv:physics/0503191.
- [25] Belle Collaboration, M.-C. Chang, et al., Observation of the decay $B^0 \rightarrow J/\psi \eta$, Phys. Rev. Lett. 98 (2007) 131803, arXiv:hep-ex/0609047.
- [26] M. Pivk, F.R. Le Diberder, sPlot: a statistical tool to unfold data distributions, Nucl. Instrum. Meth. A 555 (2005) 356, arXiv:physics/0402083.
- [27] LHCb Collaboration, R. Aaij, et al., Measurement of the $B_s^0 \rightarrow J/\psi \bar{K}^{*0}$ branching fraction and angular amplitudes, Phys. Rev. D 86 (2012) 071102(R), arXiv:1208.0738.
- [28] LHCb Collaboration, R. Aaij, et al., Measurement of the $B_s^0 \rightarrow J/\psi K_S^0$ branching fraction, Phys. Lett. B 713 (2012) 172, arXiv:1205.0934.

LHCb Collaboration

R. Aaij⁴⁰, C. Abellan Beteta^{35,n}, B. Adeva³⁶, M. Adinolfi⁴⁵, C. Adrover⁶, A. Affolder⁵¹, Z. Ajaltouni⁵, J. Albrecht⁹, F. Alessio³⁷, M. Alexander⁵⁰, S. Ali⁴⁰, G. Alkhazov²⁹, P. Alvarez Cartelle³⁶, A.A. Alves Jr.^{24,37}, S. Amato², S. Amerio²¹, Y. Amhis⁷, L. Anderlini^{17,f}, J. Anderson³⁹, R. Andreassen⁵⁹, R.B. Appleby⁵³, O. Aquines Gutierrez¹⁰, F. Archilli¹⁸, A. Artamonov³⁴, M. Artuso⁵⁶, E. Aslanides⁶, G. Auriemma^{24,m}, S. Bachmann¹¹, J.J. Back⁴⁷, C. Baesso⁵⁷, V. Balagura³⁰, W. Baldini¹⁶, R.J. Barlow⁵³, C. Barschel³⁷, S. Barsuk⁷, W. Barter⁴⁶, Th. Bauer⁴⁰, A. Bay³⁸, J. Beddow⁵⁰, F. Bedeschi²², I. Bediaga¹, S. Belogurov³⁰, K. Belous³⁴, I. Belyaev^{30,*}, E. Ben-Haim⁸, M. Benayoun⁸, G. Bencivenni¹⁸, S. Benson⁴⁹, J. Benton⁴⁵, A. Berezhnoy³¹, R. Bernet³⁹, M.-O. Bettler⁴⁶, M. van Beuzekom⁴⁰, A. Bien¹¹, S. Bifani¹², T. Bird⁵³, A. Bizzeti^{17,h}, P.M. Bjørnstad⁵³, T. Blake³⁷, F. Blanc³⁸, J. Blouw¹¹, S. Blusk⁵⁶, V. Bocci²⁴, A. Bondar³³, N. Bondar²⁹, W. Bonivento¹⁵, S. Borghi⁵³, A. Borgia⁵⁶, T.J.V. Bowcock⁵¹, E. Bowen³⁹, C. Bozzi¹⁶, T. Brambach⁹, J. van den Brand⁴¹, J. Bressieux³⁸, D. Brett⁵³, M. Britsch¹⁰, T. Britton⁵⁶, N.H. Brook⁴⁵, H. Brown⁵¹, I. Burducea²⁸, A. Bursche³⁹, G. Busetto^{21,q}, J. Buytaert³⁷, S. Cadeddu¹⁵, O. Callot⁷, M. Calvi^{20,j}, M. Calvo Gomez^{35,n}, A. Camboni³⁵, P. Campana^{18,37}, A. Carbone^{14,c}, G. Carboni^{23,k}, R. Cardinale^{19,i}, A. Cardini¹⁵, H. Carranza-Mejia⁴⁹, L. Carson⁵², K. Carvalho Akiba², G. Casse⁵¹, M. Cattaneo³⁷, Ch. Cauet⁹, M. Charles⁵⁴, Ph. Charpentier³⁷, P. Chen^{3,38}, N. Chiapolini³⁹, M. Chrzaszcz²⁵, K. Ciba³⁷, X. Cid Vidal³⁶, G. Ciezarek⁵², P.E.L. Clarke⁴⁹, M. Clemencic³⁷, H.V. Cliff⁴⁶, J. Closier³⁷, C. Coca²⁸, V. Coco⁴⁰, J. Cogan⁶, E. Cogneras⁵, P. Collins³⁷, A. Comerma-Montells³⁵, A. Contu¹⁵, A. Cook⁴⁵, M. Coombes⁴⁵,

S. Coquereau⁸, G. Corti³⁷, B. Couturier³⁷, G.A. Cowan³⁸, D. Craik⁴⁷, S. Cunliffe⁵², R. Currie⁴⁹, C. D'Ambrosio³⁷, P. David⁸, P.N.Y. David⁴⁰, I. De Bonis⁴, K. De Bruyn⁴⁰, S. De Capua⁵³, M. De Cian³⁹, J.M. De Miranda¹, M. De Oyanguren Campos^{35,o}, L. De Paula², W. De Silva⁵⁹, P. De Simone¹⁸, D. Decamp⁴, M. Deckenhoff⁹, L. Del Buono⁸, D. Derkach¹⁴, O. Deschamps⁵, F. Dettori⁴¹, A. Di Canto¹¹, H. Dijkstra³⁷, M. Dogaru²⁸, S. Donleavy⁵¹, F. Dordei¹¹, A. Dosil Suárez³⁶, D. Dossett⁴⁷, A. Dovbnya⁴², F. Dupertuis³⁸, R. Dzhelyadin³⁴, A. Dziurda²⁵, A. Dzyuba²⁹, S. Easo^{48,37}, U. Egede⁵², V. Egorychev³⁰, S. Eidelman³³, D. van Eijk⁴⁰, S. Eisenhardt⁴⁹, U. Eitschberger⁹, R. Ekelhof⁹, L. Eklund⁵⁰, I. El Rifai⁵, Ch. Elsasser³⁹, D. Elsby⁴⁴, A. Falabella^{14,e}, C. Färber¹¹, G. Fardell⁴⁹, C. Farinelli⁴⁰, S. Farry¹², V. Fave³⁸, D. Ferguson⁴⁹, V. Fernandez Albor³⁶, F. Ferreira Rodrigues¹, M. Ferro-Luzzi³⁷, S. Filippov³², C. Fitzpatrick³⁷, M. Fontana¹⁰, F. Fontanelli^{19,i}, R. Forty³⁷, O. Francisco², M. Frank³⁷, C. Frei³⁷, M. Frosini^{17,f}, S. Furcas²⁰, E. Furfaro²³, A. Gallas Torreira³⁶, D. Galli^{14,c}, M. Gandelman², P. Gandini⁵⁴, Y. Gao³, J. Garofoli⁵⁶, P. Garosi⁵³, J. Garra Tico⁴⁶, L. Garrido³⁵, C. Gaspar³⁷, R. Gauld⁵⁴, E. Gersabeck¹¹, M. Gersabeck⁵³, T. Gershon^{47,37}, Ph. Ghez⁴, V. Gibson⁴⁶, V.V. Gligorov³⁷, C. Göbel⁵⁷, D. Golubkov³⁰, A. Golutvin^{52,30,37}, A. Gomes², H. Gordon⁵⁴, M. Grabalosa Gándara⁵, R. Graciani Diaz³⁵, L.A. Granado Cardoso³⁷, E. Graugés³⁵, G. Graziani¹⁷, A. Grecu²⁸, E. Greening⁵⁴, S. Gregson⁴⁶, O. Grünberg⁵⁸, B. Gui⁵⁶, E. Gushchin³², Yu. Guz³⁴, T. Gys³⁷, C. Hadjivasiliou⁵⁶, G. Haefeli³⁸, C. Haen³⁷, S.C. Haines⁴⁶, S. Hall⁵², T. Hampson⁴⁵, S. Hansmann-Menzemer¹¹, N. Harnew⁵⁴, S.T. Harnew⁴⁵, J. Harrison⁵³, T. Hartmann⁵⁸, J. He⁷, V. Heijne⁴⁰, K. Hennessy⁵¹, P. Henrard⁵, J.A. Hernando Morata³⁶, E. van Herwijnen³⁷, E. Hicks⁵¹, D. Hill⁵⁴, M. Hoballah⁵, C. Hombach⁵³, P. Hopchev⁴, W. Hulsbergen⁴⁰, P. Hunt⁵⁴, T. Huse⁵¹, N. Hussain⁵⁴, D. Hutchcroft⁵¹, D. Hynds⁵⁰, V. Iakovenko⁴³, M. Idzik²⁶, P. Ilten¹², R. Jacobsson³⁷, A. Jaeger¹¹, E. Jans⁴⁰, P. Jaton³⁸, F. Jing³, M. John⁵⁴, D. Johnson⁵⁴, C.R. Jones⁴⁶, B. Jost³⁷, M. Kaballo⁹, S. Kandybei⁴², M. Karacson³⁷, T.M. Karbach³⁷, I.R. Kenyon⁴⁴, U. Kerzel³⁷, T. Ketel⁴¹, A. Keune³⁸, B. Khanji²⁰, O. Kochebina⁷, I. Komarov^{38,31}, R.F. Koopman⁴¹, P. Koppenburg⁴⁰, M. Korolev³¹, A. Kozlinskiy⁴⁰, L. Kravchuk³², K. Kreplin¹¹, M. Kreps⁴⁷, G. Krocker¹¹, P. Krokovny³³, F. Kruse⁹, M. Kucharczyk^{20,25,j}, V. Kudryavtsev³³,

T. Kvaratskheliya^{30,37}, V.N. La Thi³⁸, D. Lacarrere³⁷, G. Lafferty⁵³,
A. Lai¹⁵, D. Lambert⁴⁹, R.W. Lambert⁴¹, E. Lanciotti³⁷,
G. Lanfranchi^{18,37}, C. Langenbruch³⁷, T. Latham⁴⁷, C. Lazzeroni⁴⁴,
R. Le Gac⁶, J. van Leerdam⁴⁰, J.-P. Lees⁴, R. Lefèvre⁵, A. Leflat^{31,37},
J. Lefrançois⁷, S. Leo²², O. Leroy⁶, B. Leverington¹¹, Y. Li³,
L. Li Gioi⁵, M. Liles⁵¹, R. Lindner³⁷, C. Linn¹¹, B. Liu³, G. Liu³⁷,
J. von Loeben²⁰, S. Lohn³⁷, J.H. Lopes², E. Lopez Asamar³⁵,
N. Lopez-March³⁸, H. Lu³, D. Lucchesi^{21,q}, J. Luisier³⁸, H. Luo⁴⁹,
F. Machefert⁷, I.V. Machikhiliyan^{4,30}, F. Maciuc²⁸, O. Maev^{29,37},
S. Malde⁵⁴, G. Manca^{15,d}, G. Mancinelli⁶, U. Marconi¹⁴, R. Märki³⁸,
J. Marks¹¹, G. Martellotti²⁴, A. Martens⁸, L. Martin⁵⁴,
A. Martín Sánchez⁷, M. Martinelli⁴⁰, D. Martinez Santos⁴¹,
D. Martins Tostes², A. Massafferri¹, R. Matev³⁷, Z. Mathe³⁷,
C. Matteuzzi²⁰, E. Maurice⁶, A. Mazurov^{16,32,37,e}, J. McCarthy⁴⁴,
R. McNulty¹², A. McNab⁵³, B. Meadows^{59,54}, F. Meier⁹, M. Meissner¹¹,
M. Merk⁴⁰, D.A. Milanes⁸, M.-N. Minard⁴, J. Molina Rodriguez⁵⁷,
S. Monteil⁵, D. Moran⁵³, P. Morawski²⁵, M.J. Morello^{22,s},
R. Mountain⁵⁶, I. Mous⁴⁰, F. Muheim⁴⁹, K. Müller³⁹, R. Muresan²⁸,
B. Muryn²⁶, B. Muster³⁸, P. Naik⁴⁵, T. Nakada³⁸, R. Nandakumar⁴⁸,
I. Nasteva¹, M. Needham⁴⁹, N. Neufeld³⁷, A.D. Nguyen³⁸,
T.D. Nguyen³⁸, C. Nguyen-Mau^{38,p}, M. Nicol⁷, V. Niess⁵, R. Niet⁹,
N. Nikitin³¹, T. Nikodem¹¹, A. Nomerotski⁵⁴, A. Novoselov³⁴,
A. Oblakowska-Mucha²⁶, V. Obraztsov³⁴, S. Oggero⁴⁰, S. Ogilvy⁵⁰,
O. Okhrimenko⁴³, R. Oldeman^{15,37,d}, M. Orlandea²⁸,
J.M. Otalora Goicochea², P. Owen⁵², B.K. Pal⁵⁶, A. Palano^{13,b},
M. Palutan¹⁸, J. Panman³⁷, A. Papanestis⁴⁸, M. Pappagallo⁵⁰,
C. Parkes⁵³, C.J. Parkinson⁵², G. Passaleva¹⁷, G.D. Patel⁵¹, M. Patel⁵²,
G.N. Patrick⁴⁸, C. Patrignani^{19,i}, C. Pavel-Nicorescu²⁸,
A. Pazos Alvarez³⁶, A. Pellegrino⁴⁰, G. Penso^{24,l}, M. Pepe Altarelli³⁷,
S. Perazzini^{14,c}, D.L. Perego^{20,j}, E. Perez Trigo³⁶,
A. Pérez-Calero Yzquierdo³⁵, P. Perret⁵, M. Perrin-Terrin⁶, G. Pessina²⁰,
K. Petridis⁵², A. Petrolini^{19,i}, A. Phan⁵⁶, E. Picatoste Olloqui³⁵,
B. Pietrzyk⁴, T. Pilař⁴⁷, D. Pinci²⁴, S. Playfer⁴⁹, M. Plo Casasus³⁶,
F. Polci⁸, S. Polikarpov³⁰, G. Polok²⁵, A. Poluektov^{47,33}, E. Polycarpo²,
D. Popov¹⁰, B. Popovici²⁸, C. Potterat³⁵, A. Powell⁵⁴, J. Prisciandaro³⁸,
V. Pugatch⁴³, A. Puig Navarro³⁸, G. Punzi^{22,r}, W. Qian⁴,
J.H. Rademacker⁴⁵, B. Rakotomiamanana³⁸, M.S. Rangel²,

I. Raniuk⁴², N. Rauschmayr³⁷, G. Raven⁴¹, S. Redford⁵⁴, M.M. Reid⁴⁷,
 A.C. dos Reis¹, S. Ricciardi⁴⁸, A. Richards⁵², K. Rinnert⁵¹,
 V. Rives Molina³⁵, D.A. Roa Romero⁵, P. Robbe⁷, E. Rodrigues⁵³,
 P. Rodriguez Perez³⁶, S. Roiser³⁷, V. Romanovsky³⁴, A. Romero Vidal³⁶,
 J. Rouvinet³⁸, T. Ruf³⁷, F. Ruffini²², H. Ruiz³⁵, P. Ruiz Valls^{35,o},
 G. Sabatino^{24,k}, J.J. Saborido Silva³⁶, N. Sagidova²⁹, P. Sail⁵⁰,
 B. Saitta^{15,d}, C. Salzmann³⁹, B. Sanmartin Sedes³⁶, M. Sannino^{19,i},
 R. Santacesaria²⁴, C. Santamarina Rios³⁶, E. Santovetti^{23,k},
 M. Sapunov⁶, A. Sarti^{18,l}, C. Satriano^{24,m}, A. Satta²³, M. Savrie^{16,e},
 D. Savrina^{30,31}, P. Schaack⁵², M. Schiller⁴¹, H. Schindler³⁷,
 M. Schlupp⁹, M. Schmelling¹⁰, B. Schmidt³⁷, O. Schneider³⁸,
 A. Schopper³⁷, M.-H. Schune⁷, R. Schwemmer³⁷, B. Sciascia¹⁸,
 A. Sciubba²⁴, M. Seco³⁶, A. Semennikov³⁰, K. Senderowska²⁶,
 I. Sepp⁵², N. Serra³⁹, J. Serrano⁶, P. Seyfert¹¹, M. Shapkin³⁴,
 I. Shapoval^{42,37}, P. Shatalov³⁰, Y. Shcheglov²⁹, T. Shears^{51,37},
 L. Shekhtman³³, O. Shevchenko⁴², V. Shevchenko³⁰, A. Shires⁵²,
 R. Silva Coutinho⁴⁷, T. Skwarnicki⁵⁶, N.A. Smith⁵¹, E. Smith^{54,48},
 M. Smith⁵³, M.D. Sokoloff⁵⁹, F.J.P. Soler⁵⁰, F. Soomro^{18,37}, D. Souza⁴⁵,
 B. Souza De Paula², B. Spaan⁹, A. Sparkes⁴⁹, P. Spradlin⁵⁰, F. Stagni³⁷,
 S. Stahl¹¹, O. Steinkamp³⁹, S. Stoica²⁸, S. Stone⁵⁶, B. Storaci³⁹,
 M. Straticiuc²⁸, U. Straumann³⁹, V.K. Subbiah³⁷, S. Swientek⁹,
 V. Syropoulos⁴¹, M. Szczekowski²⁷, P. Szczypka^{38,37}, T. Szumlak²⁶,
 S. T'Jampens⁴, M. Teklishyn⁷, E. Teodorescu²⁸, F. Teubert³⁷,
 C. Thomas⁵⁴, E. Thomas³⁷, J. van Tilburg¹¹, V. Tisserand⁴, M. Tobin³⁹,
 S. Tolk⁴¹, D. Tonelli³⁷, S. Topp-Joergensen⁵⁴, N. Torr⁵⁴,
 E. Tournefier^{4,52}, S. Tourneur³⁸, M.T. Tran³⁸, M. Tresch³⁹,
 A. Tsaregorodtsev⁶, P. Tsopelas⁴⁰, N. Tuning⁴⁰, M. Ubeda Garcia³⁷,
 A. Ukleja²⁷, D. Urner⁵³, U. Uwer¹¹, V. Vagnoni¹⁴, G. Valenti¹⁴,
 R. Vazquez Gomez³⁵, P. Vazquez Regueiro³⁶, S. Vecchi¹⁶, J.J. Velthuis⁴⁵,
 M. Veltri^{17,g}, G. Veneziano³⁸, M. Vesterinen³⁷, B. Viaud⁷, D. Vieira²,
 X. Vilasis-Cardona^{35,n}, A. Vollhardt³⁹, D. Volyanskyy¹⁰, D. Voong⁴⁵,
 A. Vorobyev²⁹, V. Vorobyev³³, C. Voß⁵⁸, H. Voss¹⁰, R. Waldi⁵⁸,
 R. Wallace¹², S. Wandernoth¹¹, J. Wang⁵⁶, D.R. Ward⁴⁶, N.K. Watson⁴⁴,
 A.D. Webber⁵³, D. Websdale⁵², M. Whitehead⁴⁷, J. Wicht³⁷,
 J. Wiechczynski²⁵, D. Wiedner¹¹, L. Wiggers⁴⁰, G. Wilkinson⁵⁴,
 M.P. Williams^{47,48}, M. Williams⁵⁵, F.F. Wilson⁴⁸, J. Wishahi⁹,
 M. Witek²⁵, S.A. Wotton⁴⁶, S. Wright⁴⁶, S. Wu³, K. Wyllie³⁷, Y. Xie^{49,37},

F. Xing⁵⁴, Z. Xing⁵⁶, Z. Yang³, R. Young⁴⁹, X. Yuan³, O. Yushchenko³⁴,
 M. Zangoli¹⁴, M. Zavertyaev^{10,a}, F. Zhang³, L. Zhang⁵⁶, W.C. Zhang¹²,
 Y. Zhang³, A. Zhelezov¹¹, A. Zhokhov³⁰, L. Zhong³, A. Zvyagin³⁷

¹ Centro Brasileiro de Pesquisas Físicas (CBPF), Rio de Janeiro, Brazil

² Universidade Federal do Rio de Janeiro (UFRJ), Rio de Janeiro, Brazil

³ Center for High Energy Physics, Tsinghua University, Beijing, China

⁴ LAPP, Université de Savoie, CNRS/IN2P3, Annecy-Le-Vieux, France

⁵ Clermont Université, Université Blaise Pascal, CNRS/IN2P3, LPC, Clermont-Ferrand, France

⁶ CPPM, Aix-Marseille Université, CNRS/IN2P3, Marseille, France

⁷ LAL, Université Paris-Sud, CNRS/IN2P3, Orsay, France

⁸ LPNHE, Université Pierre et Marie Curie, Université Paris Diderot, CNRS/IN2P3, Paris, France

⁹ Fakultät Physik, Technische Universität Dortmund, Dortmund, Germany

¹⁰ Max-Planck-Institut für Kernphysik (MPIK), Heidelberg, Germany

¹¹ Physikalisches Institut, Ruprecht-Karls-Universität Heidelberg, Heidelberg, Germany

¹² School of Physics, University College Dublin, Dublin, Ireland

¹³ Sezione INFN di Bari, Bari, Italy

¹⁴ Sezione INFN di Bologna, Bologna, Italy

¹⁵ Sezione INFN di Cagliari, Cagliari, Italy

¹⁶ Sezione INFN di Ferrara, Ferrara, Italy

¹⁷ Sezione INFN di Firenze, Firenze, Italy

¹⁸ Laboratori Nazionali dell'INFN di Frascati, Frascati, Italy

¹⁹ Sezione INFN di Genova, Genova, Italy

²⁰ Sezione INFN di Milano Bicocca, Milano, Italy

²¹ Sezione INFN di Padova, Padova, Italy

²² Sezione INFN di Pisa, Pisa, Italy

²³ Sezione INFN di Roma Tor Vergata, Roma, Italy

²⁴ Sezione INFN di Roma La Sapienza, Roma, Italy

²⁵ Henryk Niewodniczanski Institute of Nuclear Physics Polish Academy of Sciences, Kraków, Poland

²⁶ AGH University of Science and Technology, Kraków, Poland

²⁷ National Center for Nuclear Research (NCBJ), Warsaw, Poland

²⁸ Horia Hulubei National Institute of Physics and Nuclear Engineering, Bucharest-Magurele, Romania

²⁹ Petersburg Nuclear Physics Institute (PNPI), Gatchina, Russia

³⁰ Institute of Theoretical and Experimental Physics (ITEP), Moscow, Russia

³¹ Institute of Nuclear Physics, Moscow State University (SINP MSU), Moscow, Russia

³² Institute for Nuclear Research of the Russian Academy of Sciences (INR RAN), Moscow, Russia

³³ Budker Institute of Nuclear Physics (SB RAS) and Novosibirsk State University, Novosibirsk, Russia

³⁴ Institute for High Energy Physics (IHEP), Protvino, Russia

³⁵ Universitat de Barcelona, Barcelona, Spain

³⁶ Universidad de Santiago de Compostela, Santiago de Compostela, Spain

³⁷ European Organization for Nuclear Research (CERN), Geneva, Switzerland

³⁸ Ecole Polytechnique Fédérale de Lausanne (EPFL), Lausanne, Switzerland

³⁹ Physik-Institut, Universität Zürich, Zürich, Switzerland

⁴⁰ Nikhef National Institute for Subatomic Physics, Amsterdam, The Netherlands

⁴¹ Nikhef National Institute for Subatomic Physics and VU University Amsterdam, Amsterdam, The Netherlands

⁴² NSC Kharkiv Institute of Physics and Technology (NSC KIPT), Kharkiv, Ukraine

⁴³ Institute for Nuclear Research of the National Academy of Sciences (KINR), Kyiv, Ukraine

⁴⁴ University of Birmingham, Birmingham, United Kingdom

⁴⁵ H.H. Wills Physics Laboratory, University of Bristol, Bristol, United Kingdom

⁴⁶ Cavendish Laboratory, University of Cambridge, Cambridge, United Kingdom

⁴⁷ Department of Physics, University of Warwick, Coventry, United Kingdom

⁴⁸ STFC Rutherford Appleton Laboratory, Didcot, United Kingdom

⁴⁹ School of Physics and Astronomy, University of Edinburgh, Edinburgh, United Kingdom

⁵⁰ School of Physics and Astronomy, University of Glasgow, Glasgow, United Kingdom

⁵¹ Oliver Lodge Laboratory, University of Liverpool, Liverpool, United Kingdom

⁵² Imperial College London, London, United Kingdom

⁵³ School of Physics and Astronomy, University of Manchester, Manchester, United Kingdom

⁵⁴ Department of Physics, University of Oxford, Oxford, United Kingdom

⁵⁵ Massachusetts Institute of Technology, Cambridge, MA, United States

⁵⁶ Syracuse University, Syracuse, NY, United States

⁵⁷ Pontifícia Universidade Católica do Rio de Janeiro (PUC-Rio), Rio de Janeiro, Brazil^t

⁵⁸ Institut für Physik, Universität Rostock, Rostock, Germany^u

⁵⁹ University of Cincinnati, Cincinnati, OH, United States^v

* Corresponding author.

E-mail address: Ivan.Belyaev@itep.ru (I. Belyaev).

^a P.N. Lebedev Physical Institute, Russian Academy of Science (LPI RAS), Moscow, Russia.

^b Università di Bari, Bari, Italy.

^c Università di Bologna, Bologna, Italy.

^d Università di Cagliari, Cagliari, Italy.

^e Università di Ferrara, Ferrara, Italy.

^f Università di Firenze, Firenze, Italy.

^g Università di Urbino, Urbino, Italy.

^h Università di Modena e Reggio Emilia, Modena, Italy.

ⁱ Università di Genova, Genova, Italy.

^j Università di Milano Bicocca, Milano, Italy.

^k Università di Roma Tor Vergata, Roma, Italy.

^l Università di Roma La Sapienza, Roma, Italy.

^m Università della Basilicata, Potenza, Italy.

ⁿ LIFAELS, La Salle, Universitat Ramon Llull, Barcelona, Spain.

^o IFIC, Universitat de Valencia-CSIC, Valencia, Spain.

^p Hanoi University of Science, Hanoi, Viet Nam.

^q Università di Padova, Padova, Italy.

^r Università di Pisa, Pisa, Italy.

^s Scuola Normale Superiore, Pisa, Italy.

^t Associated to: Universidade Federal do Rio de Janeiro (UFRJ), Rio de Janeiro, Brazil.

^u Associated to: Physikalisches Institut, Ruprecht-Karls-Universität Heidelberg, Heidelberg, Germany.

^v Associated to: Syracuse University, Syracuse, NY, United States.